

## TITLE

Transcriptome and fatty-acid signatures of adipocyte hypertrophy and its non-invasive MR-based characterization in human adipose tissue

## AUTHORS

Julius Honecker<sup>1,#,\*</sup>, Stefan Ruschke<sup>2,#</sup>, Claudine Seeliger<sup>1</sup>, Samantha Laber<sup>3</sup>, Sophie Strobel<sup>3</sup>, Priska Pröll<sup>4</sup>, Christoffer Nellaker<sup>5,6</sup>, Cecilia M. Lindgren<sup>3,5</sup>, Ulrich Kulozik<sup>4</sup>, Josef Ecker<sup>7</sup>, Dimitrios C. Karampinos<sup>2,8</sup>, Melina Claussnitzer<sup>3,9,10,‡</sup>, Hans Hauner<sup>1,11,‡,\*</sup>

## AFFILIATIONS

<sup>1</sup> Else Kröner-Fresenius-Center for Nutritional Medicine, Chair of Nutritional Medicine, TUM School of Life Sciences, Technical University of Munich, Gregor-Mendel-Straße 2, 85354 Freising-Weihenstephan, Germany

<sup>2</sup> Department of Diagnostic and Interventional Radiology, School of Medicine, Technical University of Munich, Munich, Germany

<sup>3</sup> Broad Institute of MIT and Harvard, Cambridge, MA, USA

<sup>4</sup> Food- and Bioprocess Engineering, TUM School of Life Sciences, Technical University of Munich, Weihenstephaner Berg 1, 85354 Freising, Germany.

<sup>5</sup> Big Data Institute, Li Ka Shing Centre for Health Information and Discovery, University of Oxford, Oxford OX3 7FZ, UK.

<sup>6</sup> Nuffield Department of Women's and Reproductive Health, University of Oxford, Women's Centre, John Radcliffe Hospital, Oxford, UK

<sup>7</sup> ZIEL - Institute for Food & Health, Research Group Lipid Metabolism, Technical University of Munich, Freising, Germany.

<sup>8</sup> Munich Institute of Biomedical Engineering, Technical University of Munich, Munich, Germany

<sup>9</sup> Center for Genomic Medicine and Endocrine Division, Massachusetts General Hospital, Boston, MA, USA

<sup>10</sup> Harvard Medical School, Harvard University, Boston, MA, USA

<sup>11</sup> Institute for Nutritional Medicine, School of Medicine, Technical University of Munich, Georg-Brauchle-Ring 62, 80992 Munich, Germany

# These authors contributed equally

‡ Senior author

## \* Corresponding authors contact details:

Else Kröner-Fresenius-Center for Nutritional Medicine, Chair of Nutritional Medicine, TUM School of Life Sciences, Technical University of Munich, Phone: +498161712001

*E-mail addresses:* julius.honecker@tum.de (J.H.), hans.hauner@tum.de (H.H.)

SUPPLEMENTARY FIGURES

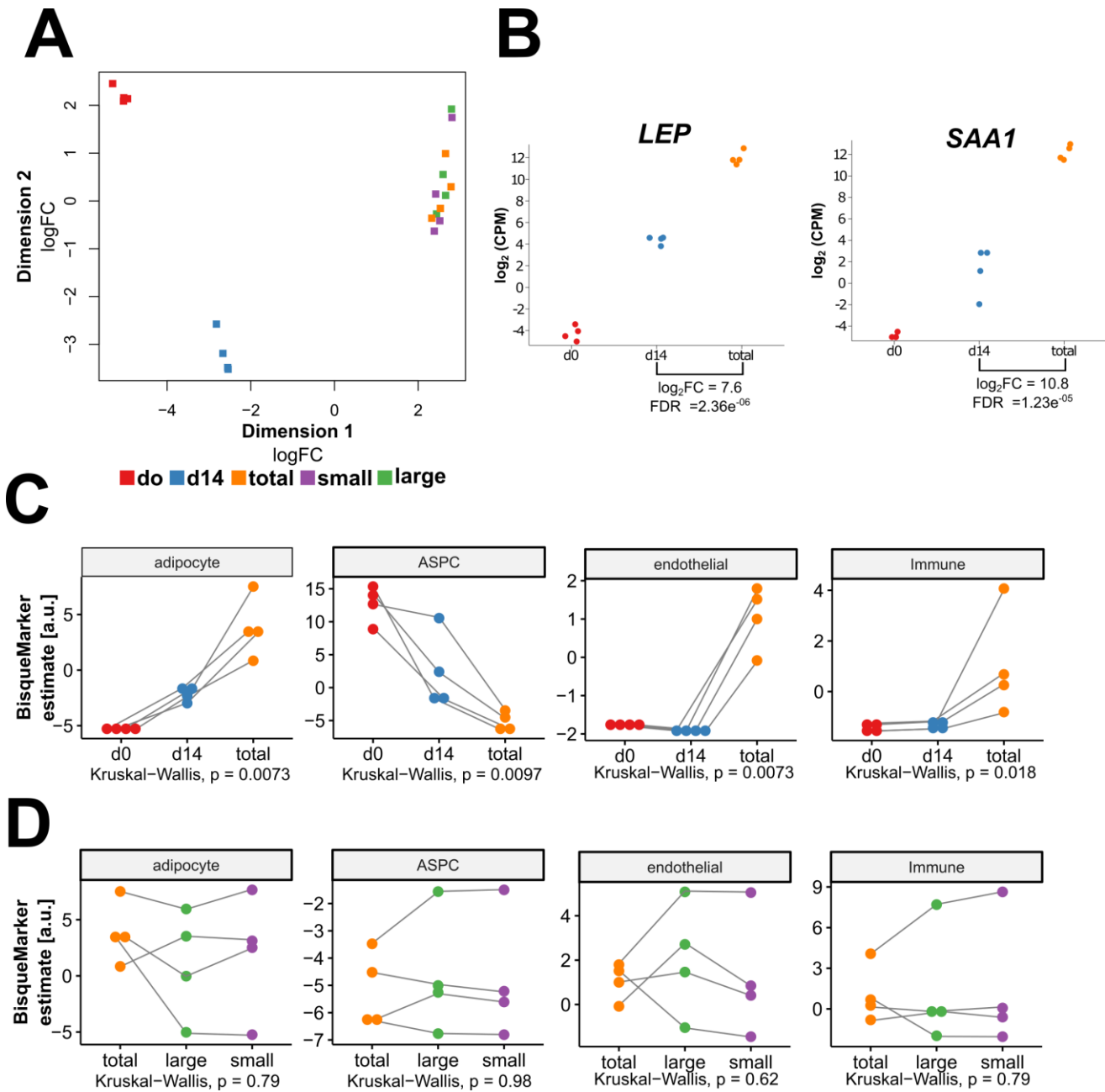


**Figure S1:** Quality and purity of mature, size-separated adipocytes

(A) Multidimensional scaling plot comparing in-vitro cultured preadipocytes on day 0 and d14 with the total, small and large mature adipocyte fraction from the same donor.

(B) Expression of adipocyte marker genes in preadipocytes and mature adipocytes

(C) BisqueMarker based gene deconvolution displaying relative differences in abundances of different cell types between preadipocytes and mature adipocytes. Samples originating from the same donor are interconnected.

(D) BisqueMarker based gene deconvolution displaying relative differences in abundances of different cell types between fractionated mature adipocytes. Samples originating from the same donor are interconnected.

All samples originate from a total of four female donors where mature adipocytes and preadipocytes were isolated in parallel. Marker genes used for Bisque deconvolution originate from a recent adipose tissue single cell sequencing publication by Emont et al.. (1, 2)

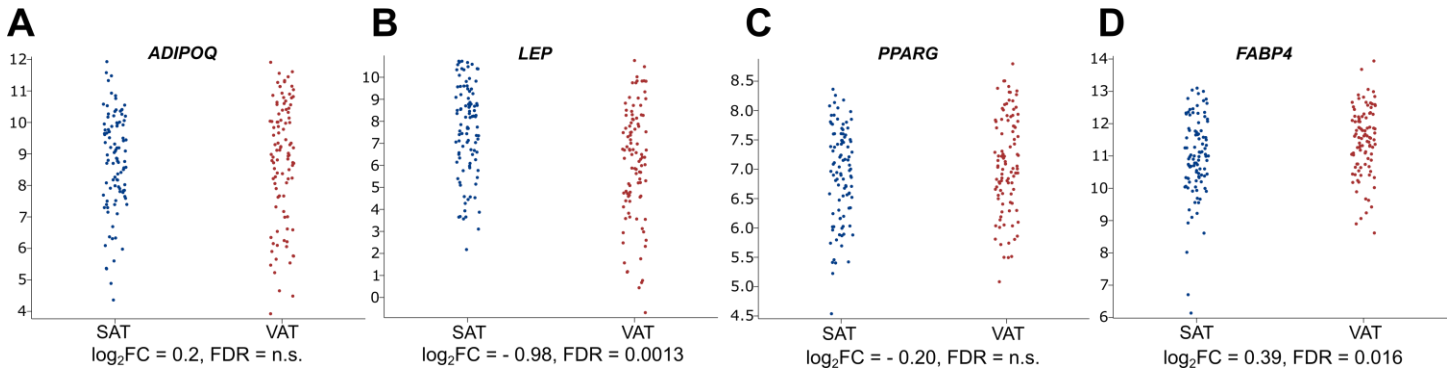


**Figure S2:** Expression of adipogenic marker genes in GTEx SAT and VAT samples.

- (A) Adiponectin
- (B) Leptin
- (C) Peroxisome proliferator-activated receptor gamma
- (D) Fatty acid binding protein 4

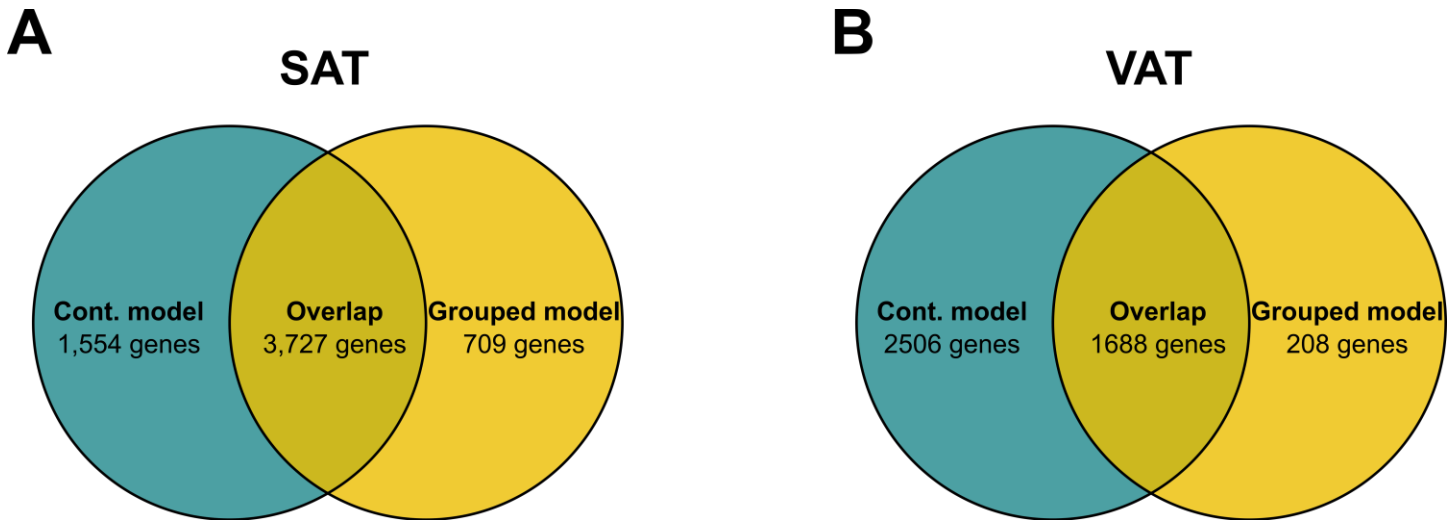


**Figure S3:** Number of differentially expressed genes in relationship to the applied differential expression model in GTEx samples (continuous vs. grouped)

- (A) In SAT 1,554 genes were unique for the continuous model (turquoise) while 709 genes were differentially expressed solely in the grouped model (yellow). Both models shared significant differential expression (FDR < 0.05) of 3,727 genes.
- (B) In VAT 2,506 genes were unique for the continuous model (turquoise) while 208 genes were differentially expressed solely in the grouped model (yellow). Both models shared significant differential expression (FDR < 0.05) of 1,688 genes.

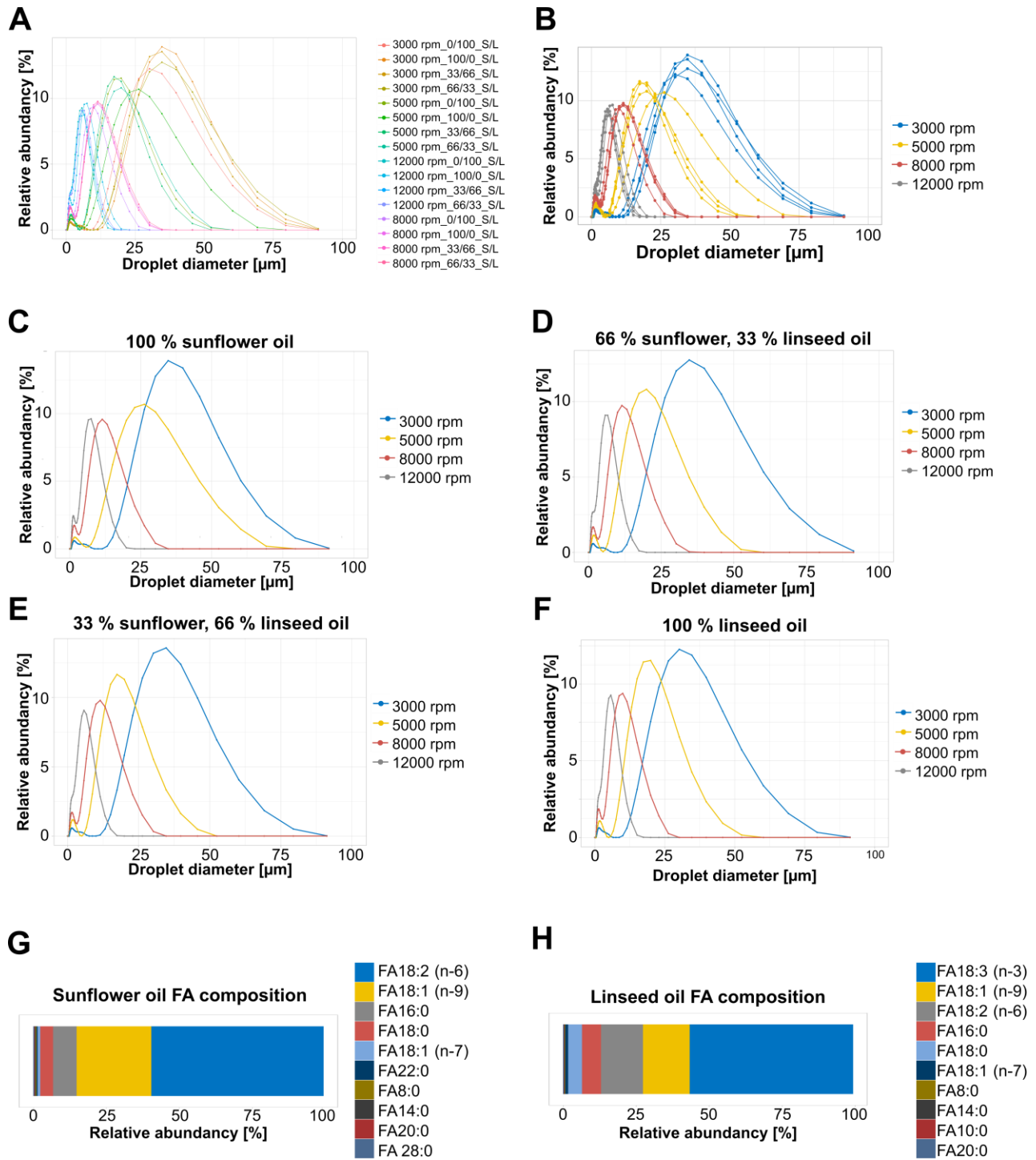


**Figure S4:** Characterization of water-fat phantoms

(A) Density plots from all water-fat phantoms.

(B) Density plots from all water-fat phantoms colored according to stirrer rpm.

(C) Density plots from the 100 % sunflower oil water-fat phantoms.

(D) Density plots from the 66 % sunflower 33 % linseed oil water-fat phantoms.

(E) Density plots from the 33 % sunflower 66 % linseed oil water-fat phantoms.

(F) Density plots from the 100 % linseed oil water-fat phantoms.

(G) Top ten most abundant fatty acid species in sunflower oil.

(H) Top ten most abundant fatty acid species in linseed oil.

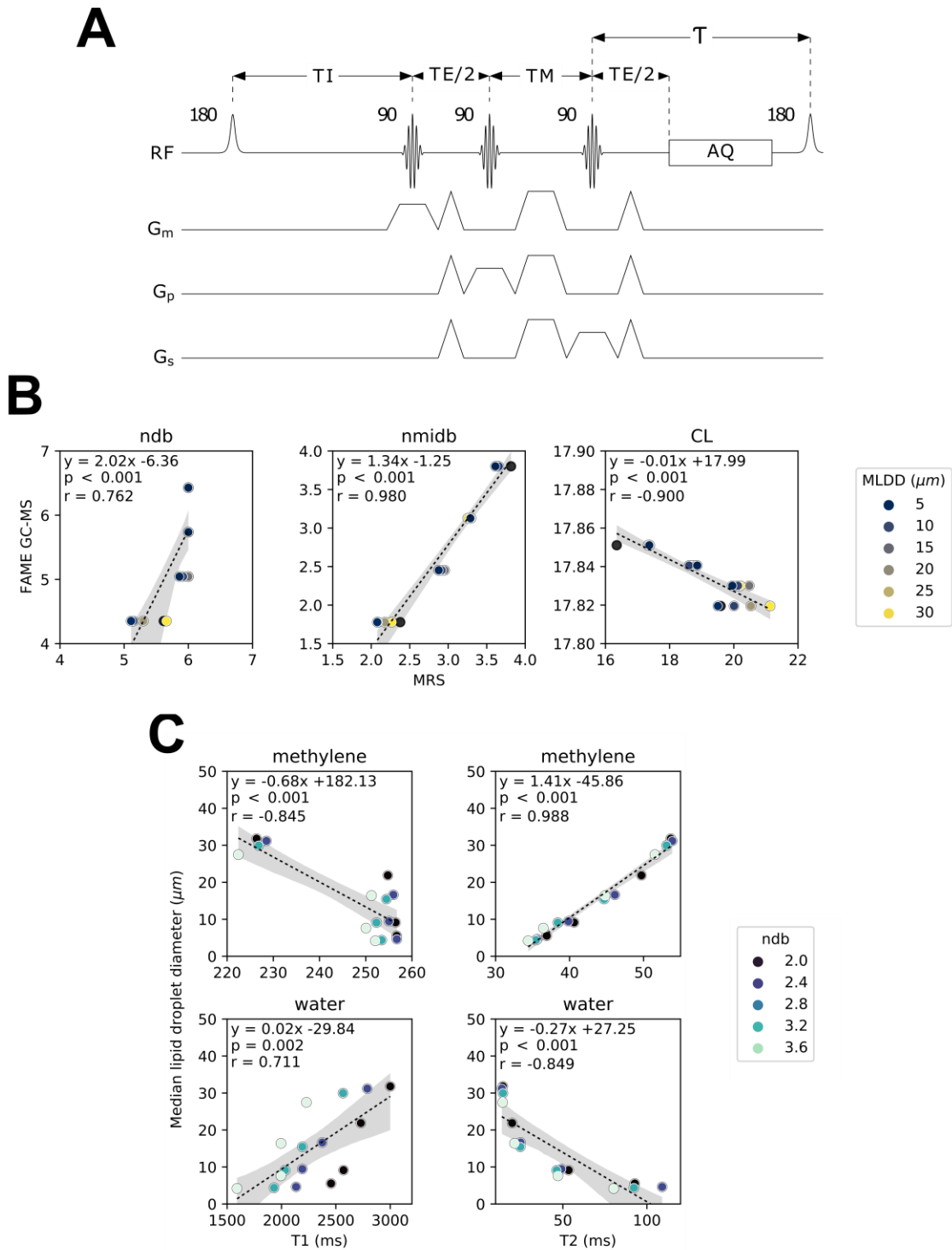


**Figure S5: MRS-based characterization of fatty acid composition and lipid droplet size in phantoms**

(A) MRS pulse sequence diagram of the single-voxel short-TR multi-TI multi-TE (SHORTIE) STEAM sequence. The sequence consists of a regular single-voxel STEAM sequence pattern with a minimal TR (constant recovery delay  $\tau$ ) combined with a non-selective 180-degree inversion RF-pulse. (B) Linear regression plots from the phantom experiment: GC-MS-based vs. MRS-based quantification of the FA characteristics ndb, nmiddb, CL. The negative correlation for CL ( $n = 16$ ,  $r = -0.900$ ,  $p < 0.001$ , pearson correlation) is considered an artifact arising from the difficulty of its accurate modelling and quantification in MRS. MLDD, median lipid droplet diameter. (C) Linear regression plots ( $n = 16$ , pearson correlation) from the phantom experiment of the median lipid droplet diameter vs. the T1 and T2 relaxation of methylene and water, respectively. Very strong correlation between the median lipid droplet diameter and methylene T2 relaxation ( $r = 0.988$ ,  $p < 0.001$ ) independent from the fatty acid unsaturation suggests that methylene T2 is a promising indirect measure of lipid droplet size.

## SUPPLEMENTARY TABLES

**Table S1:** Phenotype data, obtained sample types, and measured outcome variables of subjects that were included in the study.

Cohort	n [male/female]	Age [years]	BMI [kg/m <sup>2</sup> ]	Sample types	Outcome variables
GTEx SAT	153 100/53	20 – 29: 9 (5.9 %) 30 – 39: 11 (7.2. %) 40 – 49: 16 (10.5 %) 50 – 59: 46 (30.1 %) 60 – 69: 69 (45.1 %) 70 – 79: 2 (1.3 %)	N/A	WAT biopsies	RNA-Seq Adipocyte size
GTEx VAT	141 92/49	20 – 29: 10 (7.1 %) 30 – 39: 10 (7.1 %) 40 – 49: 16 (11.3 %) 50 – 59: 52 (36.9 %) 60 – 69: 49 (34.8 %) 70 – 79: 4 (2.8 %)	N/A	WAT biopsies	RNA-Seq Adipocyte size
GTEx Paired	99 64/35	20 – 29: 8 (8.1 %) 30 – 39: 8 (8.1 %) 40 – 49: 11 (11.1 %) 50 – 59: 35 (35.4 %) 60 – 69: 35 (35.4 %) 70 – 79: 2( 2.0 %)	N/A	WAT biopsies	RNA-Seq Adipocyte size
Liposuction	4 0/4	39 ± 10	27.4 ± 5.8 1 N/A	Mature adipocytes separated by size	RNA-Seq Adipocyte size
Fatty acids SAT	22 1/21	45 ± 12	32.6 ± 6.7 1 N/A	WAT biopsies	FAME GC-MS Adipocyte size
Fatty acids VAT	12 5/7	53 ± 15	36.0 ± 11.4 1 N/A	WAT biopsies	FAME GC-MS Adipocyte size
Fatty acids Paired	7 2/5	46 ± 12	40.7 ± 7.6 1 N/A	WAT biopsies	FAME GC-MS Adipocyte size
MRS SAT	16 16/0	44 ± 12	30.6 ± 4.6	WAT biopsies	MRS-derived FA profile Methylene relaxation
MRS VAT	5 3/2	51 ± 14	34.7 ± 11.4	WAT biopsies	MRS- derived FA profile Methylene relaxation

Data is given as means ± SD. Age from GTEx individuals is specified as count (%) in 10-year brackets. GTEx, Genotype-Tissue Expression project; SAT, subcutaneous adipose tissue; VAT, visceral adipose tissue; MRS, magnetic resonance spectroscopy; FAME, fatty-acid methyl ester; GC-MS, Gas chromatography–mass spectrometry

**Table S2:** Bin and depot specific GTEX phenotypes and adipocyte sizes

Bin	SAT				VAT			
	<i>Small</i>	<i>Medium</i>	<i>Large</i>	<i>X-Large</i>	<i>Small</i>	<i>Medium</i>	<i>Large</i>	<i>X-Large</i>
<b>n</b>	20	49	56	28	41	49	40	11
<b>Mean Area</b> ± <b>SD [μm<sup>2</sup>]</b>	1,383 ± 241	2,261 ± 230	3,055 ± 270	3,797 ± 235	1,089 ± 240	2,043 ± 326	2,947 ± 255	3,860 ± 335
<b>Area range</b> <b>min – max [μm<sup>2</sup>]</b>	907 – 1,759	1,790 – 2,598	2,618 – 3,468	3,487 – 4,325	482 – 1,503	1,556 – 2,540	2,570 – 3,403	3,580 – 4,612
<b>Mean Diameter</b> ± <b>SD [μm]</b>	41.96 ± 17.52	53.65 ± 17.11	62.37 ± 18.54	69.53 ± 17.30	37.24 ± 17.48	51.00 ± 20.37	61.26 ± 18.02	70.10 ± 20.65
<b>Diameter range</b> <b>min – max [μm]</b>	33.98 – 47.32	47.74 – 57.51	57.74 – 66.45	66.63 – 74.21	24.77 – 43.75	44.51 – 56.87	57.2 – 65.82	67.51 – 76.63
<b>Sex (Male/Female)</b>	14/6	28/21	39/17	19/9	22/19	30/19	29/11	11/0
<b>Age 20-29 [n/%]</b>	3 (15%)	4 (8.2%)	2 (3.6%)	0 (0%)	8 (20%)	2 (4.1%)	0 (0%)	0 (0%)
<b>Age 30-39 [n/%]</b>	2 (10%)	1 (2.0%)	7 (12%)	1 (3.6%)	4 (9.8%)	1 (2.0%)	3 (7.5%)	2 (18%)
<b>Age 40-49 [n/%]</b>	2 (10%)	6 (12%)	7 (12%)	1 (3.6%)	5 (12%)	7 (14%)	4 (10%)	0 (0%)
<b>Age 50-59 [n/%]</b>	7 (35%)	14 (29%)	17 (30%)	8 (29%)	13 (32%)	16 (33%)	17 (42%)	6 (55%)
<b>Age 60-69 [n/%]</b>	6 (30%)	24 (49%)	21 (38%)	18 (64%)	11 (27%)	21 (43%)	14 (35%)	3 (27%)
<b>Age 70-79 [n/%]</b>	0 (0%)	0 (0%)	2 (3.6%)	0 (0%)	0 (0%)	2 (4.1%)	2 (5.0%)	0 (0%)

Data is given as means ± SD. Age from GTEX individuals is specified as count (%) in 10 year brackets. Individuals were assigned to one of four bins with equally spaced adipocyte area intervals (small, medium, large, X-large). SAT, subcutaneous adipose tissue; VAT, visceral adipose tissue. Mean adipocyte diameter was calculated from adipocyte area estimates assuming spherical shape.

**Table S3:** Adipocyte diameter and area of FAME GC-MS samples

	<b>SAT FAME GC-MS</b>	<b>VAT FAME GC-MS</b>
<b>n</b>	22	12
<b>Mean Area</b> ± <b>SD [<math>\mu\text{m}^2</math>]</b>	3,457 ± 1638	3,715 ± 1070
<b>Area range min – max [<math>\mu\text{m}^2</math>]</b>	1,307 – 6,410	2,092 – 5,544
<b>Mean Diameter</b> ± <b>SD [<math>\mu\text{m}</math>]</b>	59.59 ± 15.36	63.63 ± 9.23
<b>Diameter range min – max [<math>\mu\text{m}</math>]</b>	36.74 – 85.92	48.23 – 77.06

FAME, fatty-acid methyl ester;

GC-MS, Gas chromatography–mass spectrometry

**Table S4:** Adipocyte diameter and area of MRS samples

	<b>SAT MRS*</b>	<b>VAT MRS</b>
<b>n</b>	27	5
<b>Mean Diameter</b> ± <b>SD [<math>\mu\text{m}</math>]</b>	52.7 ± 12.1	65.5 ± 7.7
<b>Diameter range mean min – max [<math>\mu\text{m}</math>]</b>	32.3 – 76.4	55.6 – 77.3
<b>Median Diameter</b> ± <b>SD [<math>\mu\text{m}</math>]</b>	52.4 ± 14.5	67.6 ± 9.1
<b>Diameter range median min – max [<math>\mu\text{m}</math>]</b>	25.9 – 78.4	58.6 – 83.7
<b>Mean Area</b> ± <b>SD [<math>\mu\text{m}^2</math>]</b>	2,697 ± 1,207	3,931 ± 993
<b>Area range mean min – max [<math>\mu\text{m}^2</math>]</b>	1050 – 5308	2,826 - 5533
<b>Median Area</b> ± <b>SD [<math>\mu\text{m}^2</math>]</b>	2,320 ± 1,241	3,650 ± 1,018
<b>Area range median min – max [<math>\mu\text{m}^2</math>]</b>	526 – 4,827	2,699 – 5,499

\* A total of 27 SAT samples were derived from 16 individual donors. Multiple SAT samples from the same donor originate from the abdominal, gluteal and thigh area. MRS, magnetic resonance spectroscopy; SAT, subcutaneous adipose tissue; VAT, visceral adipose tissue



**Table S5:** MRS signal fitting model consisting of in total eleven frequency components: 10 triglyceride frequencies and 1 water frequency. Using triglyceride-model-constraints and relaxation constraints for the fat frequencies lead to a reduction of model parameters resulting in a total of 21 degrees of freedom (DOF). Parameter bounds are given in square brackets, e.g. [lower bound; upper bound]. a.u., arbitrary unit.

	Triglycerides										Water
	methyl	methylene	$\beta$ -carboxyl	$\alpha$ -olefinic	$\alpha$ -carboxyl	diallylic	glycerol	glycerol	glycerol	olefinic	
ref. frequency (ppm)	0.90	1.30	1.61	2.03	2.26	2.79	4.15	4.30	5.23	5.31	4.67
$p_i$ (a.u.)	4 DOF: ndb [0;6], nmid [0;4], CL [10;40], scaling-factor [0;100]										1 DOF: water [0;100]
$d_i$ ( $s^{-1}$ )		1 DOF: methylene [0;25]	1 DOF: all triglyceride frequencies except methylene [0;25]								1 DOF water [0;25]
$g_i$ ( $s^{-2}$ )		1 DOF: methylene [0;25]	1 DOF: all triglyceride frequencies except methylene [0;25]								1 DOF water [0;25]
$\omega_i$ (ppm)	1 DOF: all triglyceride frequencies [-0.2;0.2]										1 DOF: water [-0.2;0.2]
$\varphi$ (rad)	1 DOF: all frequencies [-0.2;0.2]										
$T_{1,i}$ (s)	1 DOF: methyl [-0.1;2]	1 DOF: methylene [-0.1;2]	1 DOF: all triglyceride frequencies except methyl and methylene [-0.1;2]								1 DOF: water [-0.1;2]
$T_{2,i}$ (s)		1 DOF: methylene [0.005;0.7]	1 DOF: all triglyceride except methylene [0.005;0.7]								1 DOF: water [0.005;0.7]

**Table S6:** GTEx differential expression and gene set enrichment analysis results for the comparison between subcutaneous and visceral adipose tissue.

**Due to size, the table is deposited as a separate .xlsx file**

**Table S7:** GTEx differential expression and gene set enrichment results for the analysis regarding subcutaneous adipocyte area displayed either as a categorical or continuous variable.

**Due to size, the table is deposited as a separate .xlsx file**

**Table S8:** GTEx differential expression and gene set enrichment results for the analysis regarding visceral adipocyte area displayed either as a categorical or continuous variable.

**Due to size, the table is deposited as a separate .xlsx file**

**Table S9:** Tabular overview from the BATLAS analysis for the depot and size bin-specific changes in estimated brown adipocyte content as well as brown and white marker genes.

	<b>% Change in brown adipocyte content predicted by BATLAS</b>	<b>BATLAS BAT marker genes with a FDR &lt; 0.05</b>	<b>BATLAS WAT marker genes with a FDR &lt; 0.05</b>
<b>SAT vs VAT</b>	+ 6.13 %	5 ↓ / 61 ↑	9 ↓ / 5 ↑
<b>SAT</b> <b>Bin<sub>small</sub> vs- bin<sub>X-Large</sub></b>	- 8.79 %	60 ↓ / 0 ↑	6 ↓ / 2 ↑
<b>VAT</b> <b>Bin<sub>small</sub> vs- bin<sub>X-Large</sub></b>	- 13.57 %	42 ↓ / 0 ↑	1 ↓ / 1 ↑

BATLAS is a web tool used to estimate brown adipocyte content in human or mouse tissue based on RNA-Seq data (Perdikari et al, 2018, Cell Reports; <https://shiny.hest.ethz.ch/BATLAS/>)

**Table S10:** GTEx differential expression and gene set enrichment results for the analysis regarding size-separated mature adipocytes

**Due to size, the table is deposited as a separate .xlsx file**

**Table S11:** Lipid droplet sizes of water-fat phantoms

Revolutions per minute [rpm]	Mixing ratio Sunflower/Linseed	Diameter First decile [ $\mu\text{m}$ ]	Diameter Median [ $\mu\text{m}$ ]	Diameter Ninth decile [ $\mu\text{m}$ ]
3000	100/0	17.31	31.80	50.76
	66/33	16.34	31.19	51.94
	33/66	16.42	29.97	48.50
	0/100	13.93	27.48	46.64
5000	100/0	8.28	21.88	39.54
	66/33	3.37	16.62	29.86
	33/66	3.17	15.45	26.85
	0/100	5.56	16.41	28.59
8000	100/0	1.65	9.14	17.47
	66/33	1.68	9.46	17.92
	33/66	1.62	9.10	17.20
	0/100	1.40	7.62	14.71
12000	100/0	1.19	5.54	10.47
	66/33	1.19	4.63	9.03
	33/66	1.21	4.36	8.57
	0/100	1.19	4.20	8.12

**Table S12:** Fatty acid composition of sunflower and linseed oil

Sample	ndb	nmidb	CL	SFA [0-1]	UFA [0-1]	MUFA [0-1]	PUFA [0-1]	n3 [0-1]	n6 [0-1]
Sunflower	4.35	1.78	17.82	0.14	0.86	0.27	0.59	6.99e <sup>-04</sup>	0.59
Linseed	6.43	3.80	17.85	0.12	0.88	0.17	0.70	0.56	0.14

ndb, mean number of double bounds per triglyceride; nmidb, mean number of methylene interrupted double bounds per triglyceride; CL, mean fatty acid carbon chain length; SFA, saturated fatty acids; UFA, unsaturated fatty acids; MUFA, monounsaturated fatty acids; PUFA, polyunsaturated fatty acids; n3, omega-3 fatty acids; n-6 omega-6 fatty acids

## REFERENCES

1. Emont MP, Jacobs C, Essene AL, Pant D, Tenen D, Colletuori G, et al. A single-cell atlas of human and mouse white adipose tissue. *Nature*. 2022.
2. Jew B, Alvarez M, Rahmani E, Miao Z, Ko A, Garske KM, et al. Accurate estimation of cell composition in bulk expression through robust integration of single-cell information. *Nature communications*. 2020;11(1):1971.